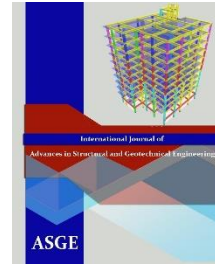




Egyptian Knowledge Bank



***International Journal of Advances in Structural
and Geotechnical Engineering***

<https://asge.journals.ekb.eg/>

Print ISSN 2785-9509

Online ISSN 2812-5142

Special Issue for ICASGE'19

***EFFECT OF COLUMN-FLANGE THICKNESS
AND BEAM-WEB SLENDERNESS RATIO ON
PANEL ZONE SHEAR STRENGTH***

Mohamed Kair, Omar Ibrahim, Ahmed Khalifa

ASGE Vol. 06 (02), pp. 89-100, 2022



EFFECT OF COLUMN-FLANGE THICKNESS AND BEAM-WEB SLENDERNESS RATIO ON PANEL ZONE SHEAR STRENGTH

Mohamed Kair¹, Omar Ibrahim², Ahmed Khalifa³

¹Teaching Assistant, Faculty of Engineering, Alexandria University, Egypt

E-mail: mohamed.aboelkhier@alexu.edu.eg

²Assistant Professor, Faculty of Engineering, Alexandria University, Egypt

E-mail: omar.ibrahim@alexu.edu.eg

³Associate Professor, Faculty of Engineering, Alexandria University, Egypt

E-mail: khalifa2030@alexu.edu.eg

ABSTRACT

Performance based design requires precise simulation of the hysteretic behavior of structural components, which depends on various structural parameters that affect the deformation and energy dissipation characteristics. Panel zone, as a component of a steel moment resisting frame (MRF), has shear yielding as its main source of energy dissipation. If properly designed, the panel zone can contribute to more than 50% of the total energy dissipation. Current design guidelines recommend the balanced design of the panel zone, while weak and strong panel zones are discouraged. The effect of the panel zone surrounding elements (column-flange thickness (CFT), and beam-web slenderness ratio (BSR)) on the panel zone shear strength has not been thoroughly investigated. Where, different studies have shown that the AISC design equation for calculating the nominal panel zone shear strength overestimates the connection shear strength, especially with thick column flanges. A parametric study (more than 1300 subassemblies) is adopted, using finite element method, to investigate the effect of CFT and BSR on the panel zone strength. The finite element models used in this study are validated using a physical experiment and the validation shows a good fit with the test results in terms of stiffness, maximum strength, total energy dissipation, and the contribution of each subassembly component (panel zone, beam, and column) to the total story drift and the total energy dissipation. The study demonstrates the considerable effect of the panel zone surrounding elements on the calculation of the panel zone shear strength.

Keywords: Panel Zone, Finite Element Analysis, Column-Flange Thickness, Shear Strength.

INTRODUCTION

Steel moment resisting frames are considered as highly ductile systems, that is why they have been widely used in many regions of high seismic activity. Building codes assign the largest force reduction factor to moment resisting frames [1, 2]. However, after the 1994 Northridge earthquake in the United States and the 1995 Kobe earthquake in Japan. Moment resisting frames did not behave as expected [3]. During the 1994 Northridge earthquake, which injured approximately 246,000 people [4], no sign of significant damages to steel building structures were immediately reported following the earthquake [3]. By the end of 1994, approximately 100 steel buildings were accidentally discovered, while solving nonstructural problems, to have structural damages.

Where, the damages were mostly reported in the beam to column connection, specifically in the lower beam flange near the face of the column flange [5].

Aftermath experiments have shown that the mean plastic rotation was 0.005 rad, which is one-sixth of the specified value of 0.03 rad. These experiments also demonstrated that the inelastic deformation of the column panel zone can hugely participate in the joint rotation, thus increasing the overall rotation capacity [6]. Current design provisions [7-9] recommend the balanced panel zone design, where panel zone is subjected to a controlled yielding. While weak panel zone increases the risk of brittle and/or ductile fracture at high connection plastic rotation [10, 11]. Moreover, a strong panel zone will remain elastic with low connection ductility, while increasing the demand of the beam plastic rotation to achieve the required story drift [12, 13]. In 1978, Krawinkler [14] proposed a mathematical model to include the flexural stiffness of the column flanges, where his model consists of an elastic perfectly plastic shear panel with four rigid boundaries surrounding it and springs at the four corners. Later, AISC seismic provisions [7, 15-22] adopted the proposed panel zone design equation by Krawinkler [14]. Current AISC seismic provision [7] takes the following forms to calculate yield panel zone shear strength (R_y) at yield panel zone distortion (γ_y) Eq.(1), and the plastic panel zone shear strength (R_p) at panel zone distortion of $4\gamma_y$ Eq.(2).

	$R_y = 0.60F_y d_c t_{pz}$	(1)
	$R_p = 0.60F_y d_c t_{pz} \left(\frac{3b_{cf} t_{cf}^2}{d_b d_c t_{pz}} \right)$	(2)
	$R_n = R_y + R_p = 0.60F_y d_c t_{pz} \left(1 + \frac{3b_{cf} t_{cf}^2}{d_b d_c t_{pz}} \right)$	(3)

Where, F_y yield stress of steel material; d_c column depth; t_{pz} panel zone thickness including doubler plate(s) if present; b_{cf} width of column flange; t_{cf} column flange thickness; d_b beam depth.

In 1978, Krawinkler [14] raised a concern that using Eq. (3) in columns with very thick flanges needs further experimental evidence to justify the calculated shear strength. He also pointed out that the stiffness and the shear capacity of the panel zone are significantly affected by the stiffness of the surrounding elements, mainly the flexural stiffness of the column flanges, the panel zone aspect ratio (d_b/d_c) and the in-plane stiffness of the beam webs alongside the panel zone. Other researchers reported the significant effect of column flange thickness (CFT) on the panel zone shear strength, where the nominal panel zone shear strength calculated using Eq. (3) overestimates the panel zone shear force at panel zone distortion of $4\gamma_y$ in case of thick column flanges [10, 13, 14, 23]. Emphasis was stated on the importance of considering the effect of thick column flanges and the beam-web slenderness ratio while estimating the panel zone shear strength [23].

To address the aforementioned challenges, this paper extensively investigates the effect of CFT and BSR on the panel zone shear strength in a balanced design panel zone. the investigation was achieved using a series of parametric studies based on finite element simulation which was validated using an experimental test carried out by Ricles et al. [24]. More than 1300 subassemblies, with mainly two variables (CFT, and BSR), were designed and analytically tested throughout this study, while other parameters such as panel zone aspect ratio (d_b/d_c) was implicitly considered through the change in column flange thickness and strong-column weak-beam ratio. Descriptive statistics are also applied to all subassemblies in this study in order to widely understand the effect of panel zone surrounding elements on its nominal shear strength.

FINITE ELEMENT SIMULATION

A finite element model (FEM) was developed using the commercial finite-element analysis software (ABAQUS 6.14). Four-node shell elements with standard integration (ABAQUS element S4) were used in the regions of finer mesh near the beam-to-column connection area and four-node shell elements with reduced integration (ABAQUS element S4R) were used in the regions

of coarse mesh. The shell elements were used instead of the solid elements because they are more capable of capturing the buckling features of the global model and provide more computational efficiency, [25], (see Fig. 1). Fig. 2 illustrates a mesh sensitivity study that was conducted to ensure the adequacy of the mesh size under monotonic load at the region of finer mesh. A mesh size of 25mm x 25mm was chosen for regions with a finer mesh, while 50mm x 25mm size was chosen for coarse mesh regions. A gradient decrease in the mesh size was applied over an adequate length of 1400mm. Fig. 3 illustrates the loading protocol as per section K2.4b in AISC 341-16 [7]. The same loading sequence used by Ricles et al. [24] in specimen (SPEC-6), which was used in the validation of the FEM. Moreover, local geometric imperfection was introduced to the FEM, using buckling mode shapes, to trigger local instabilities. The magnitude for the local imperfection equals to $d/150$, according to ASTM 2003 [26], in which, d is the cross-section depth.

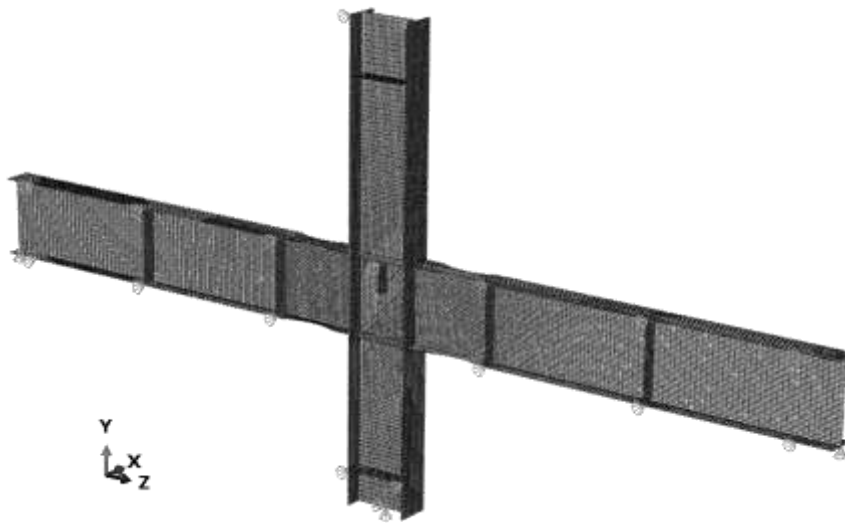


Fig. 1: Finite element model

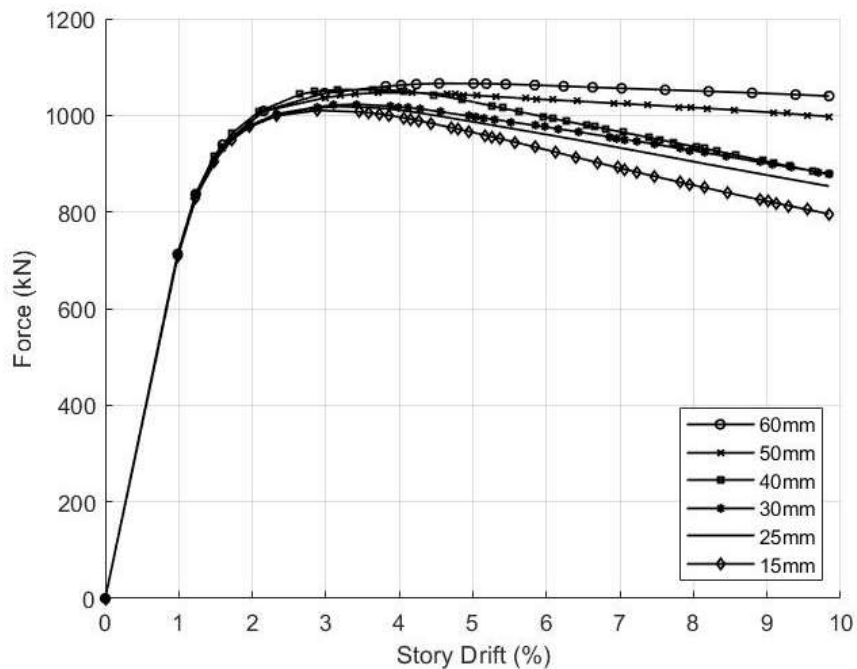


Fig. 2: Mesh sensitivity analysis

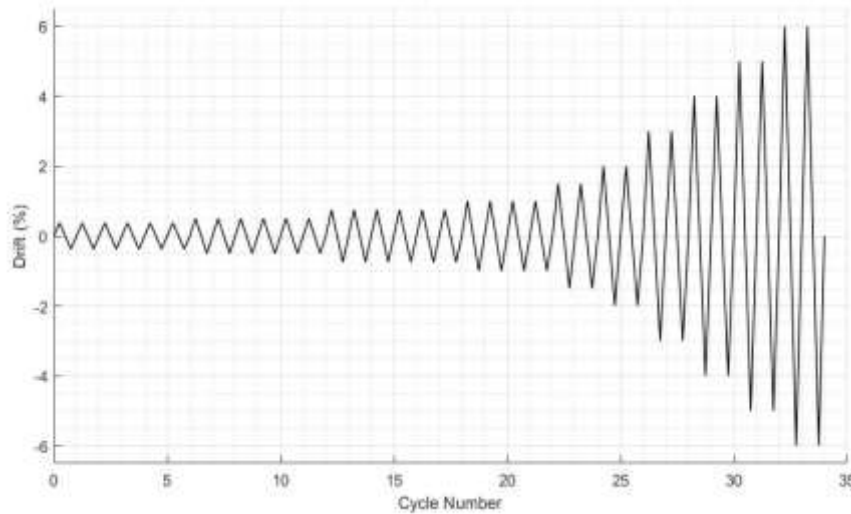


Fig. 3: Loading protocol

In addition to the modulus of elasticity and the yield stress, a combined kinematic/isotropic hardening material model was assigned to the shell element. The nonlinear kinematic hardening component is shown in Eqs. (4), and (5), which describe the translation of the yield surface in stress space through the backstress (α) [25]. The isotropic hardening component is shown in Eq. (6), which describes the change of the equivalent stress (Von Mises stress) defining the size of the yield surface (σ^0) as a function of plastic deformation [25].

	$\alpha_k = C_k \frac{1}{\sigma^0} (\sigma - \alpha) \varepsilon^{pl} - \gamma_k \alpha_k \varepsilon^{pl}$	(4)
	$\alpha = \sum_{k=1}^N \alpha_k$	(5)
	$\sigma^0 = \sigma_0 + Q_\infty (1 - e^{-b \varepsilon^{pl}})$	(6)

Where, in Eq. (4), $C_k = 3378 \text{ MPa}$ the initial kinematic hardening moduli; $\gamma_k = 20$ the rate at which kinematic hardening moduli decrease with increasing plastic deformation; σ^0 the equivalent yield stress (e.g. Von Mises stress); $\sigma_0 = 345 \text{ MPa}$ the yield stress at zero plastic strain (i.e. F_y); σ the stress tensor; and ε^{pl} the equivalent plastic strain. In Eqs. (5), $N = 1$ the number of backstresses. In Eq. (6), $Q_\infty = 90 \text{ MPa}$ the maximum change in the size of the yield surface; and $b = 12$ the rate at which the size of the yield surface changes as plastic straining develops. It should be noted that all material parameters mentioned above are for standard steel material A992 Gr. 50 and were considered according to Elkady [27].

VALIDATION OF FEM

Using SPEC-6 experimental test carried out by Ricles et al. [24], The measured maximum out-of-flatness was 3.30 millimeters which is equivalent to an imperfection magnitude $d/230$. This magnitude will only be used in the validation while $d/150$ will be used for the rest of the study. In Fig. 4, the figure presents the column tip load versus the corresponding total story drift for two FEM (imperfection $d/150$, and $d/230$), and the experimental test results. The FE models with imperfection of $d/150$ and $d/230$ reached almost 92% and 92.6% of the test peak strength, respectively, While the energy dissipated by the FE models was 95.5% and 96% of the energy dissipated by the test, respectively. It is obvious that the hysteretic behavior of the FE models with $d/150$ and $d/230$ imperfection magnitudes are almost identical. Fig. 5 (a, b, and c) shows a good agreement between the FEM and the experimental results. Where, the energy dissipated by the panel zone, beam, and column in the FEM and test (FEM-test) is 68% - 70%, 29% - 26%, and 4% - 5%, respectively, at 5% story drift.

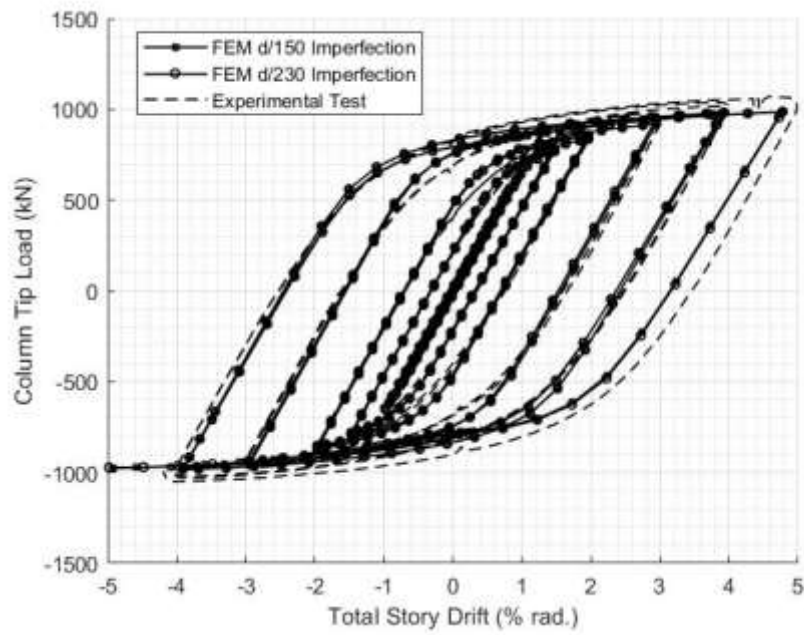


Fig. 4: Column tip load vs. Total story drift

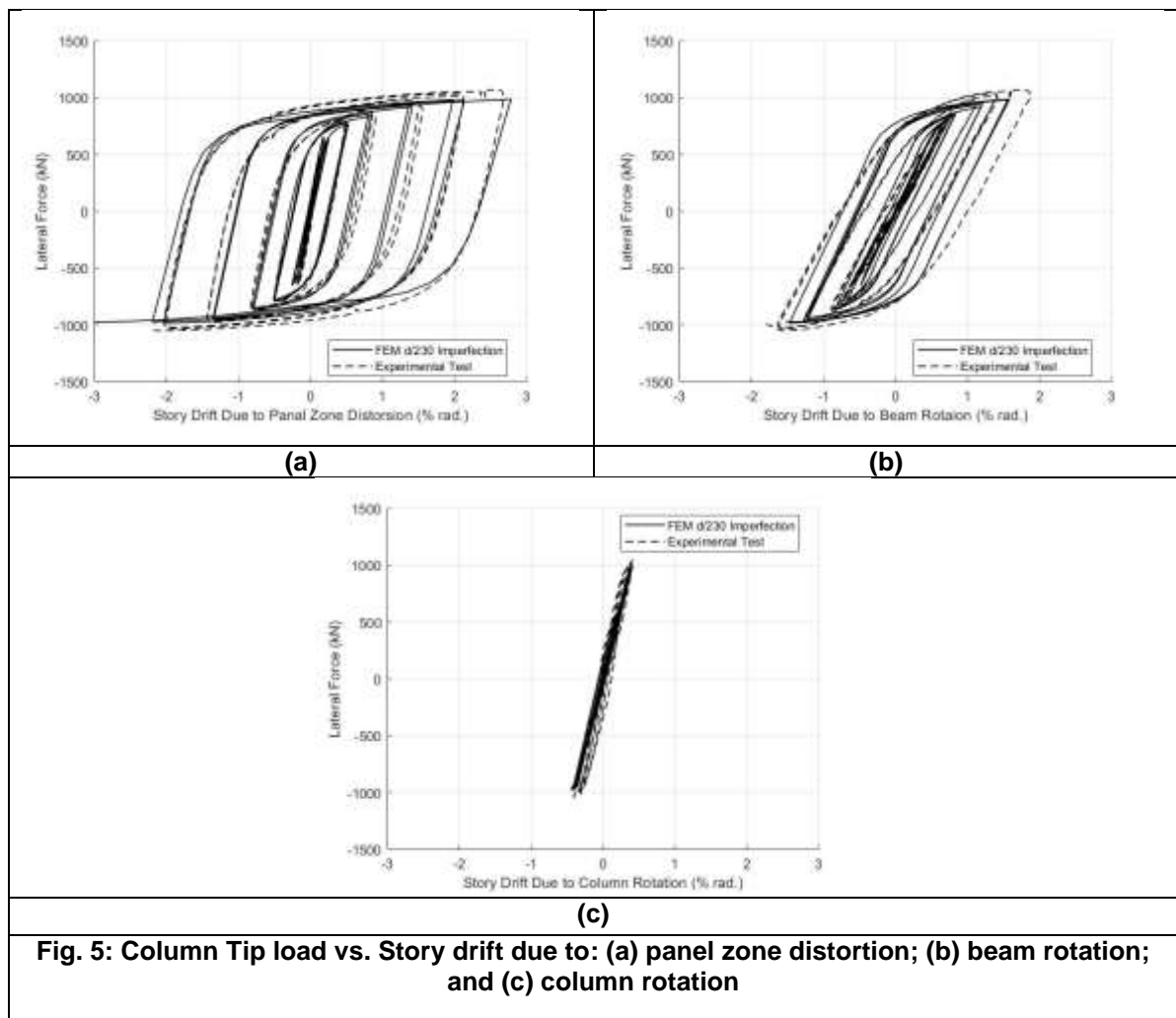


Fig. 5: Column Tip load vs. Story drift due to: (a) panel zone distortion; (b) beam rotation; and (c) column rotation

PARAMETRIC STUDY SCHEME

The validated FEM was used to develop more than 1300 subassemblies of special moment frames (SMFs) to study the effect of the column flange thickness (CFT) and beam-web slenderness ratio (BSR) on the panel zone shear force strength. Generally, as shown in Fig. 6, the subassemblies are divided into four main groups (W18W21, W21W27, W24W30 & W27W36). Each group has a distinctive beam and column depth. For example, the subassemblies group named (W24W30) has a built-up column similar to the dimensions of hot-rolled wide flange I-section (W24) and a built-up beam similar to the dimensions of hot-rolled wide flange I-section (W30). Each group is divided into two subgroups, such that (W24W30) is divided into subgroups (CFT-W24W30 & BSR-W24W30). Where, the first subgroup (CFT-W24W30) represents the subassemblies at which the variable is the column flange thickness at different sets of beam-web slenderness ratios and the second subgroup (BSR-W24W30) represents the subassemblies at which the variable is the beam-web slenderness ratio at different sets of column flange thicknesses.

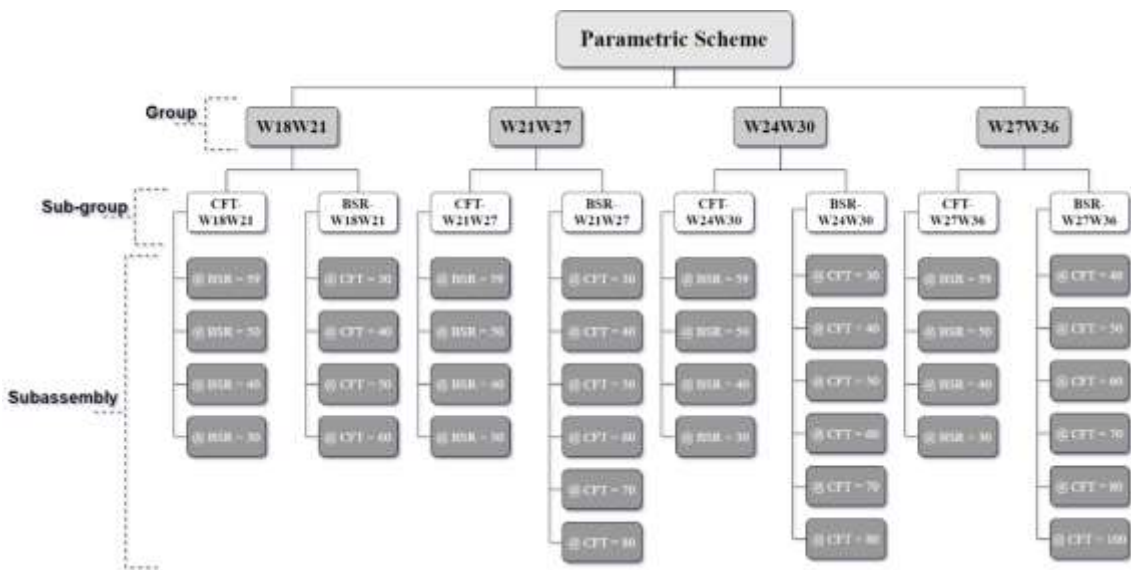


Fig. 6: Parametric plan

DATA ANALYSIS DISCUSSION

Four main subassembly groups were investigated, under monotonic loading up to 5% story drift, to observe the effect of CFT and BSR on the shear strength of the panel zone. Fig. 7 illustrates the relationship between panel zone shear force, determined using the FEM and Eq. (7), and the story drift corresponding to the panel zone distortion. The two horizontal dashed lines in Fig. 7 represent: R_n the nominal panel zone shear strength as per Eq. (3) (without resistance factor ϕ); R_m which is the measured panel zone shear force corresponding to story drift due to panel zone plastic distortion ($4\delta_y$).

$$V = \frac{\sum M_{f,m}}{d_b - t_{bf}} - V_{col} \tag{7}$$

Where, $M_{f,m}$ the measured beam bending moment at the column face calculated using beam support reaction; d_b the total beam depth; t_{bf} the beam flange thickness; and V_{col} the column shear force calculated from column horizontal reaction.

The measured panel zone nominal shear strength ratio (R_m/R_n) is deduced from Fig. 7 (henceforth called shear strength ratio), which will later be used to demonstrate whether the AISC design equation (Eq. (3)) for the panel zone shear strength overestimates ($R_m/R_n < 1.0$) or underestimates ($R_m/R_n > 1.0$) the panel zone shear force.

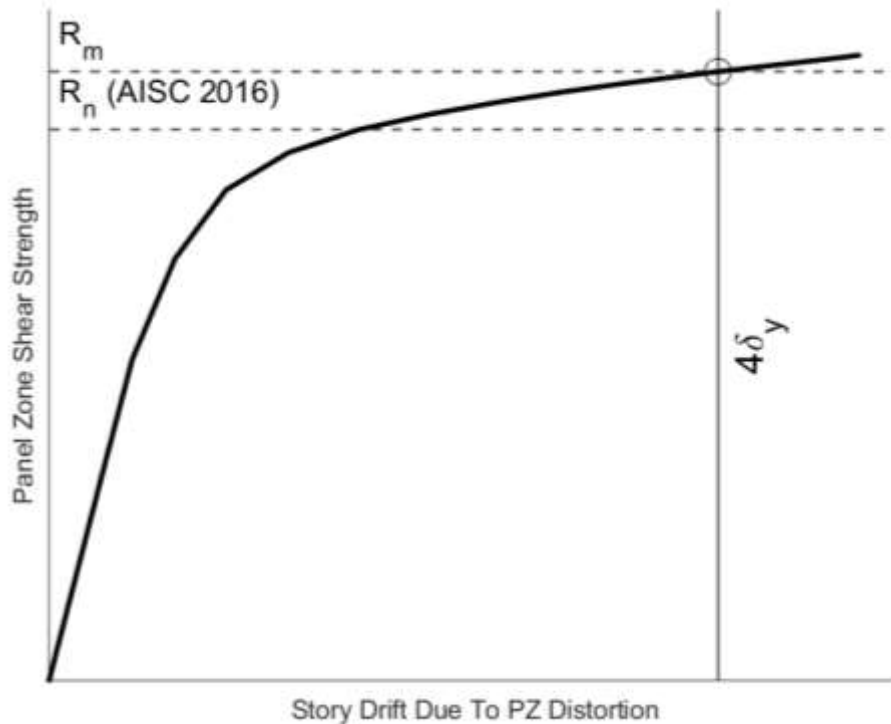


Fig. 7: Panel zone nominal shear parameters.

RESULTS

For subassembly group W18W21, a total number of (203) subassemblies were tested in this group, including (91) subassemblies for sub-group CFT-W18W21 and (112) subassemblies for sub-group BSR-W18W21. It is worth mentioning that the column web thickness changes correspondingly with the column flange thickness to achieve a constant value for the panel zone shear strength. The shear strength ratio (R_m/R_n) versus the column flange thickness (CFT) for all subassemblies in subgroup CFT-W18W21, with different BSR, are plotted in Fig. 8(a). A threshold at shear strength ratio ($R_m/R_n = 1.0$) is also plotted on the same figure. It can be observed that regardless of beam-web slenderness ratio (BSR), the AISC design equation (Eq. (3)) overestimates the panel zone shear force for column flange thicknesses greater than 44 mm, except for subassemblies with beam-web slenderness ratios (BSR) equal to 30. Eq. (3) overestimates the panel zone shear force for column flange thicknesses greater than 37 mm. Fig. 8(b) depicts the shear strength ratio (R_m/R_n) versus the beam-web slenderness ratio (BSR) for all subassemblies in subgroup BSR-W18W21 with different CFT. Fig. 8(b) emphasize on the previously stated observations. Where, in cases when the CFT is less than (37 - 44) mm, Eq. (3) works well. Although, underestimating the panel zone shear force results in an overly designed panel zone and hence more cost, especially when no doubler plate is used.

In subassembly group W21W27, a total number of (328) subassemblies were tested in this group, including (137) subassemblies for sub-group CFT-W18W21 and (191) subassemblies for sub-group BSR-W18W21. The shear strength ratio (R_m/R_n) versus the column flange thickness (CFT) for all subassemblies in subgroup CFT-W21W27, with different BSR, are plotted in Fig. 9(a). A threshold with unity shear strength ratio ($R_m/R_n = 1.0$) is also plotted on the same figure. It is obvious to say that regardless of beam-web slenderness ratio (BSR), the AISC design equation (Eq. (3)) overestimates the panel zone shear force for column flange thicknesses greater than 52 mm, while as the beam-web becomes stumpy, the thickness at which the AISC design equation starts to overestimate the panel zone nominal shear strength decreases. Where, at BSR equal to 40, Eq. (3) overestimates the panel zone shear force at CFT equal to 34 mm. Fig. 9(b), depicts the shear strength ratio (R_m/R_n) versus the beam-web slenderness ratio (BSR) for all

subassemblies in subgroup BSR-W21W27 with different CFT. Notice that when the BSR is less than 40, Eq. (3) overestimates the panel zone shear force regardless of CFT.

Subassembly group W24W30, a total number of (381) subassemblies were tested in this group, including (136) subassemblies for sub-group CFT-W24W30 and (245) subassemblies for sub-group BSR-W24W30. The shear strength ratio (R_m/R_n) versus the column flange thickness (CFT) for all subassemblies in subgroup CFT-W24W30, with different BSR, are plotted in Fig. 10(a). A threshold with unity shear strength ratio ($R_m/R_n = 1.0$) is also plotted on the same figure. It is obvious to say that regardless of beam-web slenderness ratio (BSR), the AISC design equation (Eq. (3)) overestimates the panel zone shear force for column flange thicknesses greater than 70 mm, while as the beam-web becomes stumpy, the thickness at which the AISC design equation starts to overestimate the panel zone nominal shear strength decreases. Where, at BSR equal 30, Eq. (3) overestimates the panel zone shear force at CFT equal to 61 mm. Fig. 10(b) also emphasizes the previously stated observations.

Subassembly group W27W36, a total number of (391) subassemblies were tested in this group, including (144) subassemblies for sub-group CFT-W27W36 and (247) subassemblies for sub-group BSR-W27W36. The shear strength ratio (R_m/R_n) versus the column flange thickness (CFT) for all subassemblies in subgroup CFT-W27W36, with different BSR, are plotted in Fig. 11(a). A threshold with unity shear strength ratio ($R_m/R_n = 1.0$) is also plotted on the same figure. The AISC design equation (Eq. (3)) nearly overestimates the panel zone shear force for column flange thicknesses greater than 105 mm, Since the maximum column flange thickness, allowed to be used in SMRFs, is equal to 109 mm. Then, it is fair to say that the AISC design equation underestimates the panel zone shear strength in nearly all the cases in this group. The same behavior can also be depicted in Fig. 11(b).

Fig. 12 depicts a histogram representation of the shear strength ratio (R_m/R_n) in all four groups. A total number of 1306 subassemblies have an algebraic mean equal to 1.015 and a very close median of 1.016, therefore the data are very close to symmetry. As shown in the figure, the minimum ratio is 0.78 which means that for some subassemblies Eq. (3) overestimated the panel zone shear strength by 28%. Moreover, the maximum ratio is 1.19 which means that for some subassemblies Eq. (3) underestimated the panel zone shear strength by 19%. Accordingly, a wide range (equal to 0.41) in the shear strength ratio can be found throughout the analyzed data.

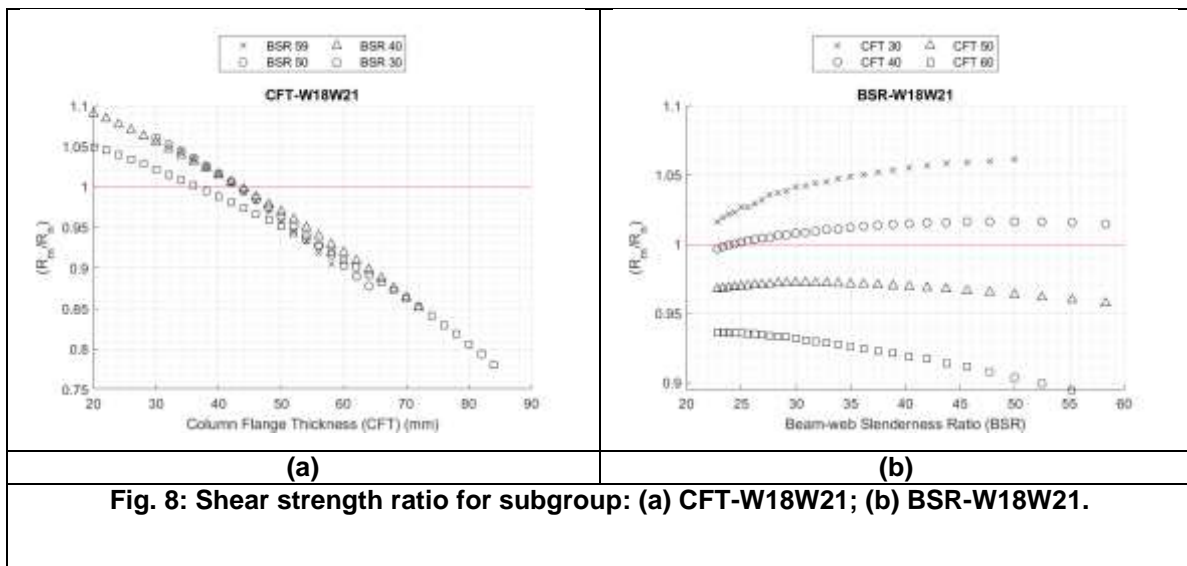


Fig. 8: Shear strength ratio for subgroup: (a) CFT-W18W21; (b) BSR-W18W21.

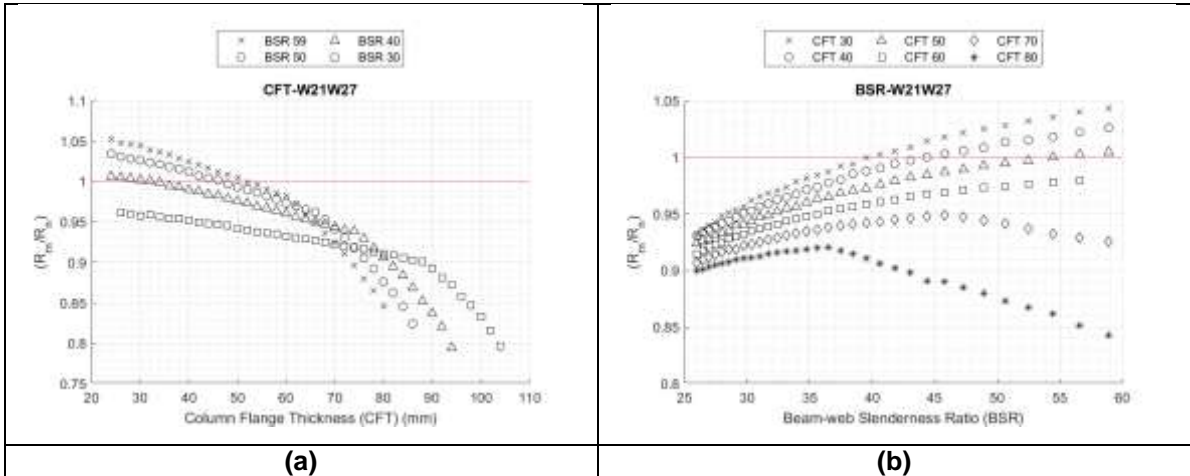


Fig. 9: Shear strength ratio for subgroup: (a) CFT-W21W27; (b) BSR-W21W27.

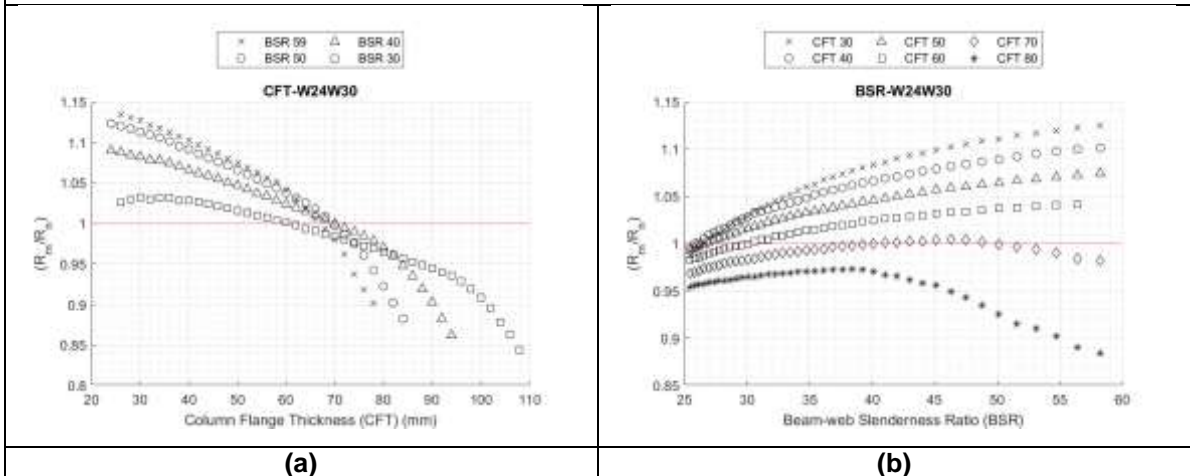


Fig. 10: Shear strength ratio for subgroup: (a) CFT-W24W30; (b) BSR-W24W30.

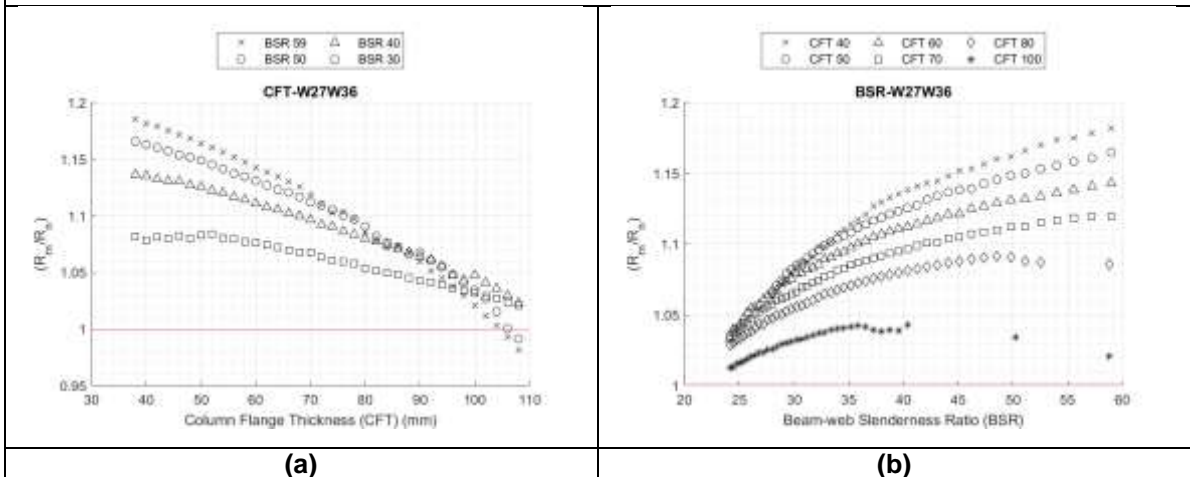


Fig. 11: Shear strength ratio for subgroup: (a) CFT-W27W36; (b) BSR-W27W36.

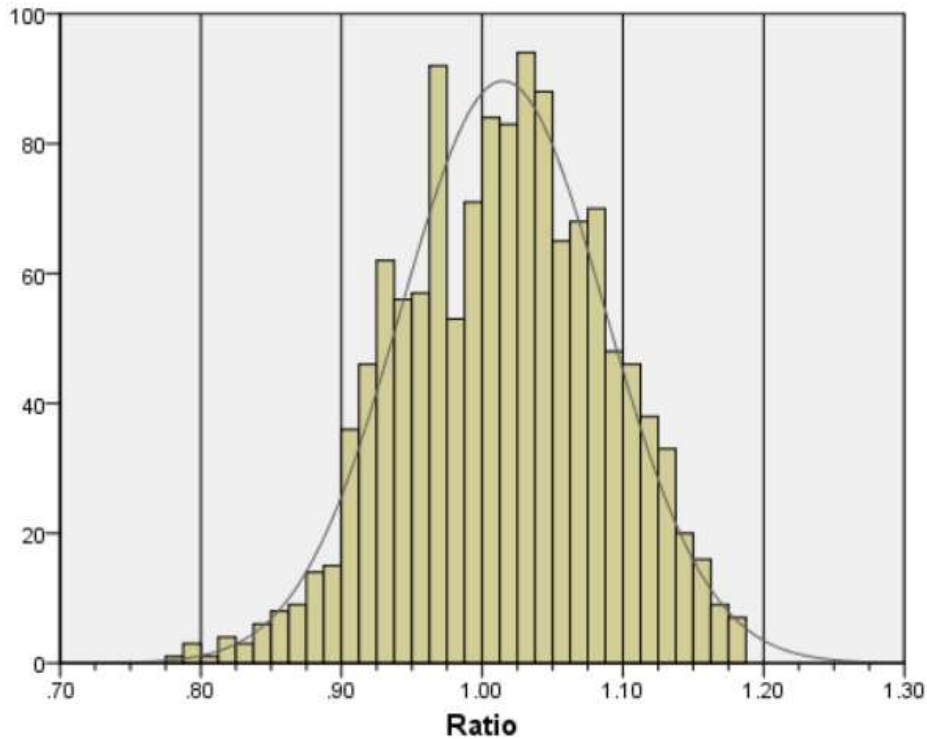


Fig. 12: Histogram of shear strength ratio.

SUMMARY AND CONCLUSION

The primary objective of this study was to develop an understanding of the effect of the panel zone surrounding elements on its shear strength, especially the column flange thickness (CFT) and the beam-web slenderness ratio (BSR), on the panel zone shear strength. More than 1300 subassemblies were tested in this study under four different main groups (W18W21, W21W27, W24W30, & W27W36).

The results show that the effect of column flange thickness on the shear strength of the panel zone is significant. Where, as the column flange thickness increases, the AISC design equation tends to overestimate the panel zone shear strength, in some cases by 22%. Beam-web slenderness ratio (BSR) also has a considerable effect on the panel zone plastic shear strength, where, as the BSR decreases, the AISC design equation tends to overestimate the panel zone.

The critical column flange thickness, at which the AISC design equation (Eq. (3)) starts to overestimate the panel zone nominal shear strength, depends on the geometry of the subassembly. Where the critical column flange thickness was equal to 44, 52, 70, and 105 mm for the groups (W18W21), (W21W27), (W24W30), and (W27W36), respectively.

REFERENCES

1. ECP., *Egyptian Code for Loads*. 2012: Arab Republic of Egypt: Housing and Building National Research Center.
2. ASCE, *ASCE/SEI 7-16 "Minimum design loads and associated criteria for buildings and other structures"*. 2016.
3. Bruneau, M., R. Sabelli, and C.-M. Uang, *Ductile Design of Steel Structures*. 2011, New York ... McGraw-Hill Professional.
4. Porter, K., K. Shoaf, and H. Seligson, *Value of Injuries in the Northridge Earthquake*. 2006.

5. Tremblay, R., et al., *Performance of steel structures during the 1994 Northridge earthquake*. Canadian journal of civil engineering. Revue canadienne de génie civil., 1995. **22**(2): p. 338.
6. Whittaker, A., A. Gilani, and V. Bertero, *Evaluation of pre-Northridge steel moment-resisting frame joints*. TAL The Structural Design of Tall Buildings, 1998. **7**(4): p. 263-283.
7. AISC, *Seismic Provisions for Structural Steel Buildings, ANSI/AISC 341-16*. 2016a, Chicago, Ill.: American Institute of Steel Construction.
8. AISC, *Specification for structural steel buildings, ANSI/AISC 360-16*. 2016c, Chicago, Ill.: American Institute of Steel Construction.
9. AISC, *Prequalified Connections for Special and Intermediate Steel Moment Frames for Seismic Applications, ANSI/AISC 358-16*. 2016b, Chicago, Ill.: American Institute of Steel Construction.
10. El-Tawil, S., et al., *Inelastic Behavior and Design of Steel Panel Zones*. Journal of Structural Engineering Journal of Structural Engineering, 1999. **125**(2): p. 183-193.
11. Gupta, A. and H. Krawinkler, *Seismic demands for performance evaluation of steel moment resisting frame structures (SAC task 5.4.3)*. 1999, Stanford, Calif.: The John A. Blume Earthquake Engineering Center.
12. Kim, S.-Y. and C.-H. Lee, *Seismic retrofit of welded steel moment connections with highly composite floor slabs*. Journal of Constructional Steel Research, 2017. **139**: p. 62-68.
13. Shin, S., *Experimental and analytical investigation of panel zone behavior in steel moment frames*. 2017.
14. Krawinkler, H., *Shear in beam-column joints in seismic design of steel frames*. Engineering Journal, 1978. **15**(3).
15. AISC, *Seismic provisions for structural steel buildings*. 2010, Chicago, Ill.: American Institute of Steel Construction.
16. AISC, *Seismic provisions for structural steel buildings (1997). Supplement no. 2. Supplement no. 2*. 2000, Chicago, Ill.: American Institute of Steel Construction.
17. AISC, *Seismic provisions for structural steel buildings (1997). Supplement no. 1. Supplement no. 1*. 1999, Chicago, Ill.: American Institute of Steel Construction.
18. AISC, *Seismic provisions for structural steel buildings*. 1992, Chicago, Ill.: American Institute of steel construction.
19. AISC, *Seismic provisions for structural steel buildings : load and resistance factor design*. 1990, Chicago: AISC.
20. AISC, *Seismic provisions for structural steel buildings*. 2002, Chicago, Ill.: American Institute of Steel Construction.
21. AISC, *Seismic provisions for structural steel buildings*. 2005, Chicago, Ill.: American Institute of Steel Construction.
22. AISC, *Seismic provisions for structural steel buildings (1997)*. 1997, Chicago, Ill.: American Institute of Steel Construction.
23. Soliman, A.A., O.A. Ibrahim, and A.M. Ibrahim, *Effect of panel zone strength ratio on reduced beam section steel moment frame connections*. Alexandria Engineering Journal Alexandria Engineering Journal, 2018. **57**(4): p. 3523-3533.
24. Ricles, J.M., et al., *Development of seismic guidelines for deep-column steel moment connections*. 2004, Bethlehem, PA: ATLSS, Lehigh University.

25. ABAQUS, *Standard User's Manual, Version 6.14*. Dassault Systèmes Simulia Corp.
26. ASTM, *Standard Specification for General Requirements for Rolled Structural Steel Bars, Plates, Shapes, and Sheet Piling*. American Society for Testing and Materials, West Conshohocken, PA. 2003.
27. Elkady, *Collapse risk assessment of steel moment resisting frames designed with deep wide-flange columns in seismic regions*. 2016, McGill University.